



Mouse Palmitoyl Protein Thioesterase: Gene Structure and Expression of cDNA

Tarja Salonen, Elina Hellsten, Nina Horelli-Kuitunen, et al.

Genome Res. 1998 8: 724-730

Access the most recent version at doi:[10.1101/gr.8.7.724](https://doi.org/10.1101/gr.8.7.724)

References This article cites 21 articles, 7 of which can be accessed free at:
<http://genome.cshlp.org/content/8/7/724.full.html#ref-list-1>

License

Email Alerting Service Receive free email alerts when new articles cite this article - sign up in the box at the top right corner of the article or [click here](#).



To subscribe to *Genome Research* go to:
<https://genome.cshlp.org/subscriptions>

Cold Spring Harbor Laboratory Press

LETTER

Mouse Palmitoyl Protein Thioesterase: Gene Structure and Expression of cDNA

Tarja Salonen,¹ Elina Hellsten,^{1,3} Nina Horelli-Kuitunen,²
Leena Peltonen,¹ and Anu Jalanko¹

¹National Public Health Institute and Institute of Biomedicine, Department of Human Molecular Genetics, University of Helsinki, FIN-00300 Helsinki, Finland; ²Helsinki University Central Hospital, Laboratory of Molecular Genetics, Meilahti Hospital, FIN-00290 Helsinki, Finland

Palmitoyl protein thioesterase (PPT) is the defective enzyme in infantile neuronal ceroid lipofuscinosis (INCL), which is a recessively inherited, progressive neurodegenerative disorder. We present here the cloning, chromosomal mapping, genomic structure, and the expression of the cDNA of mouse *PPT*. The mouse *PPT* gene spans >21 kb of genomic DNA and contains nine exons with a coding sequence of 918 bp. Fluorescence in situ hybridization to metaphase chromosomes localized the mouse *PPT* gene to the chromosome 4 conserved syntenic region with human chromosome 1p32 where the human *PPT* is located. *PPT* is expressed widely in a variety of mouse tissues. The mouse *PPT* cDNA is conserved highly with the human and rat *PPT* both at the nucleotide and amino acid sequence level. Transient expression of mouse *PPT* in COS-1 cells yielded a 38/36-kD differentially glycosylated polypeptide that was also secreted into culture media. Immunofluorescence analysis of transiently transfected HeLa cells indicated lysosomal localization of mouse *PPT*. Based on the high conservation of the gene and polypeptide structure as well as similar processing and intracellular localization, the function of *PPT* in mouse and human are likely to be very similar.

[The sequence data described in this paper have been submitted to GenBank under accession no. AF071025.]

Infantile neuronal ceroid lipofuscinosis (INCL, CLN1) is an autosomal recessive neurodegenerative disorder of childhood. The incidence of INCL is 1:20,000, and the approximated carrier frequency is 1:70 in the Finnish population. INCL is characterized by ataxia, psychomotor retardation, early visual loss, and mental retardation and leads to a vegetative state by the age of 3 yr (Santavuori et al. 1974). The life expectancy of patients is ~10 yr. The accumulation of ceroid and lipofuscin-like material can be observed in neurons and other cell types when analyzing the histopathological samples of patients (Rapola and Haltia 1973). Saposins A and D constitute the main protein components accumulating in these inclusions (Tyynelä et al. 1993). The characteristic feature in tissue pathology in INCL is the selective loss of neurons of neocortical origin. Brain stem and spinal cord are much less affected, explaining the maintenance of patients' basic functions.

The INCL locus was initially localized to human

chromosome 1p32 (Järvälä et al. 1991) and the gene coding palmitoyl protein thioesterase (PPT) was subsequently identified using positional cloning strategies (Vesa et al. 1995). PPT was originally purified from bovine brain based on its ability to remove palmitate from palmitoylated H-Ras in vitro (Camp and Hofmann 1993), but the natural substrate(s) for PPT is unknown. The human *PPT* cDNA has been cloned and characterized. *PPT* gene spans 25 kb and consists of nine exons. The cDNA sequence contains a coding region of 918 bp in addition to 5' and 3' untranslated regions. The PPT polypeptide contains 306 amino acid residues and is N-glycosylated with high-mannose-type oligosaccharides (Camp et al. 1994). The enzyme is targeted to lysosomes via the mannose 6-phosphate receptor-mediated pathway and therefore INCL disease has been classified recently as a lysosomal storage disease (Hellsten et al. 1996, Verkruyse and Hofmann 1996).

A mouse deficient in *PPT* generated by gene disruption would be a valuable tool to clarify the very special pathology of INCL focusing on the neocortical regions. Toward this goal we report the cloning and characterization of the mouse *PPT* gene and

³Present address: National Institutes of Health, Laboratory of Genetic Diseases Research, Bethesda, Maryland 20814 USA.

⁴Corresponding author.

E-MAIL anu.jalanko@ktl.fi; FAX 358-9-4744-480.

further, cloning, sequence analysis, and expression of the corresponding cDNA. The data indicate high conservation in the gene structure and chromosomal localization. Mouse *PPT* polypeptide is 84.6% homologous to human enzyme and is similarly processed and lysosomally targeted as its human counterpart.

RESULTS

Cloning and Analysis of the Mouse *PPT* Gene and cDNA

Mouse *PPT* genomic clones were isolated from a genomic library of mouse strain 129 SV in λ FIX II vector. After hybridizing with human *PPT* cDNA probe, two clones were isolated (Fig. 1), subcloned into pGEM4, and characterized in detail. Southern blot analysis with human *PPT* cDNA probes showed that λ clones contained sequence-encoding exons 2–8 but did not span exon 1. The exonic sequences of the genomic clones were obtained by initial sequencing with vector-specific primers as well as primers synthesized based on the human sequence.

To confirm the predicted mouse *PPT* coding sequence and the positions of exon/intron boundaries, RT-PCR was performed on mouse liver and brain RNA with human exon 1-specific and mouse exon 8-specific primers. The single amplification product of 918 bp was sequenced, resulting in a cDNA with an open reading frame of 306 amino acids. Exon nucleotide sequences from the genomic clones were identical (all but one nucleotide: nucleotide 378 is A in mouse kidney cDNA and G in

129SV genomic DNA) to the RT-PCR cDNA sequence. The sequence of the 5'-end of exon 1 was further specified by sequencing a PCR product amplified from mouse cDNA kidney library with T7 and mouse *PPT* exon 4a primer.

Exon-intron boundaries were clarified by comparison of the mouse genomic sequence with mouse cDNA sequence from RT-PCR. The bidirectional sequencing of exons from genomic subclones using mouse *PPT*-specific primers gave ~200 nucleotides of the intronic sequences at the exon-intron boundaries. The size of each intron was determined by PCR using exon-specific primers (Fig. 1).

Chromosomal Localization

Mouse metaphase chromosomes were hybridized with genomic mouse *PPT* clones by parallel hybridization with a λ clone specific for *COL15A1* gene as a reference clone for mouse chromosome 4 (Hägg et al. 1997). The identification of the mouse chromosomes was based on their G-banding pattern (Cowell 1984) and parallel hybridization with the reference probe. The assignment of the mouse *PPT* gene was based on specific hybridization signals on chromosome 4 band D1–3 (35 metaphases out of 40) with 80% hybridization efficiency (Fig. 2). Mouse chromosome 4, D1–3, is a syntenic region with human *PPT* gene assigned to chromosome 1p32.

cDNA and Amino Acid Analysis

Comparison of the mouse versus human and rat cDNA sequences revealed that these genes display 84.3 and 94.1% identity at the nucleotide level (Fig. 3). Also a strong amino acid sequence homology was observed between the mouse and human (84.6% identity and 96.3% similarity) and between mouse and rat *PPT* (94.4% identity and 98.3% similarity). The identity between these amino acid sequences is 100% in the acyl-CoA thioesterase consensus sequence. Mouse *PPT* contained 46 bp of 5'-untranslated region, which was sequenced both from a PCR product of a mouse kidney cDNA library and from a 5' RACE (not shown). Additionally, a 1.5-kb 3'-untranslated region could be

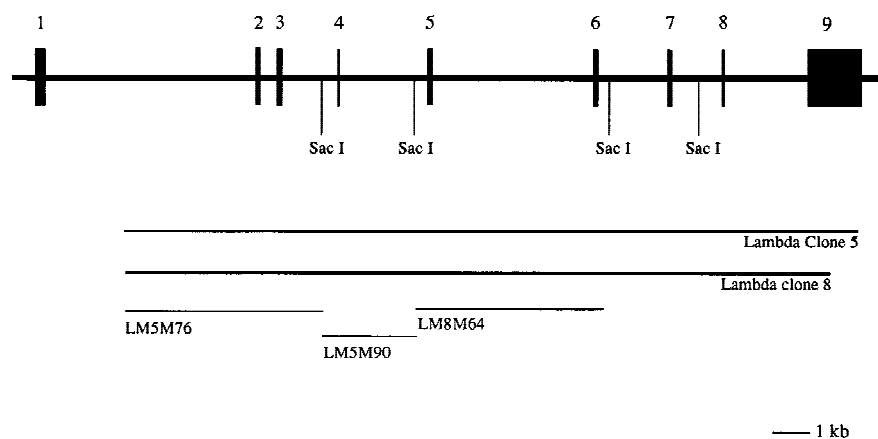


Figure 1 Structure of the mouse *PPT* gene. Diagrammatic representation of the mouse *PPT* gene and the isolated λ clones (λ M5 and λ M8). Also the subclones LM5M76, LM5M90, and LM8M64 used for FISH are marked. Restriction sites for *Sac*I are indicated on the map.

SALONEN ET AL.

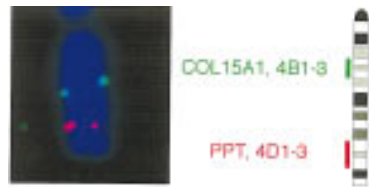


Figure 2 FISH analysis of mouse metaphase chromosomes. FISH of the mouse *PPT* gene. Examples of *PPT* signals (red) and *COL15A1* (green) on mouse chromosome 4 both represent double-detected FISH signals and a diagrammatic illustration of FISH mapping data showing mouse *PPT* on chromosome 4 band D1–3.

detected by detected by PCR analysis from the mouse kidney cDNA library. Two putative polyadenylation signals were identified at positions 1288 and 2290.

Analysis of RNA

The presence of *PPT* mRNA was demonstrated by Northern blot analysis in eight tissues examined. Highest steady-state mRNA levels were detected in testis and kidney. Heart, brain, spleen, lung, and liver showed lower, relatively similar mRNA levels, and the lowest level was found in skeletal muscle. The mouse *PPT* gives a major transcript of 2.65 kb and a smaller 1.85 kb transcription product when hybridized with a cDNA probe containing the coding region of mouse *PPT* (Fig. 4). Exceptionally to other tissues the 1.85-kb mRNA was the major transcript found in testis. The *in vivo* finding of two mRNAs supports the cDNA sequence data in which two putative polyadenylation sites 1 kb apart could be detected.

Intracellular Synthesis and Maturation of the Mouse *PPT*

To study the intracellular processing and transport of the mouse *PPT* enzyme, the cDNA was subcloned into the pCMV5 expression vector. Immediately after synthesis, mouse *PPT* could be detected as four bands of apparent molecular masses of 32, 34, 36, and 38 kD. Intracellular mouse *PPT* was processed to a 36/38-kD doublet mature form when chase time was extended to 2 hr. The enzyme was also detected extracellularly after a 2-hr chase period. In the media, mouse *PPT* was always found as a 36- and 38-kD doublet. As compared to fully mature human *PPT* (35/37 kD) the mouse enzyme seemed to migrate slightly more slowly on the SDS-polyacrylamide gels (Fig. 5A,B). The ratio between the extracellular

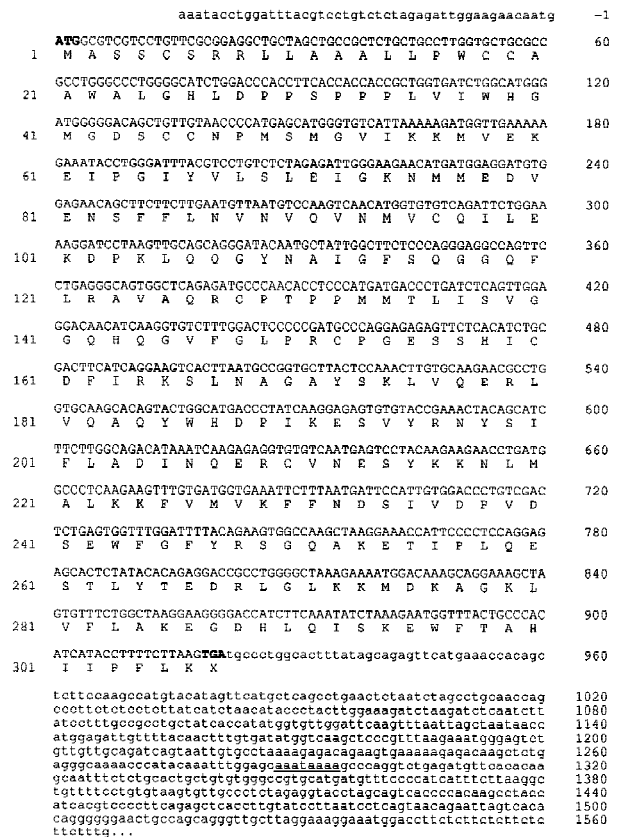


Figure 3 The nucleotide sequence of mouse *PPT* cDNA. The open reading frame encoded by the gene is in uppercase letters. Nucleotide positions are at right. The amino acid sequence starting with initiator methionine is numbered at left. The first polyadenylation signal is underlined.

and intracellular *PPT* polypeptides is approximately four times lower in mouse *PPT* than in human *PPT*.

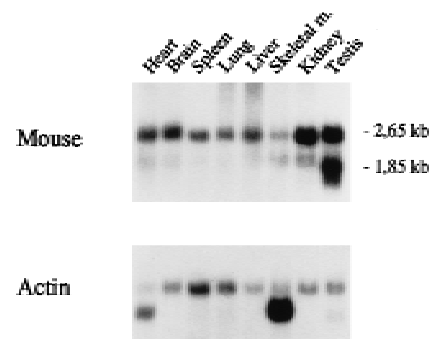


Figure 4 Northern blot analysis of *PPT* mRNA in different mouse tissues. (Lane 1) Heart; (lane 2) brain; (lane 3) spleen; (lane 4) lung; (lane 5) liver; (lane 6) skeletal muscle; (lane 7) kidney; (lane 8) testis. Sizes of the *PPT* transcripts are indicated. The filter was probed with 32 P-labeled *PPT* cDNA. (Bottom) β -Actin control probe hybridized of the same filter as used in top.

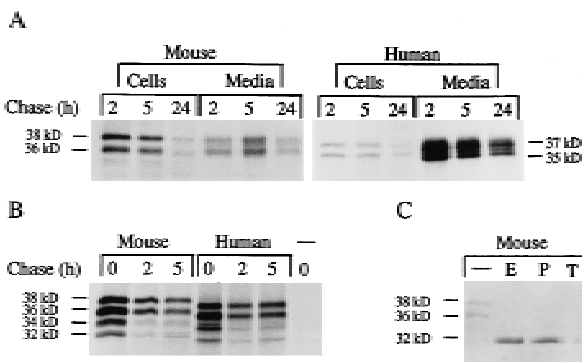


Figure 5 SDS-PAGE analysis of mouse and human PPT transfected in COS-1 cells and immunoprecipitated with anti-human PPT antibody. (A) Cells transfected with mouse PPT construct, pulse labeled for 1 hr and chased at 2, 5, and 24 hr. Both cells and media were immunoprecipitated. As a control cells transfected with a human PPT construct are shown at *right*. (B) Maturation of the intracellular mouse and human PPT polypeptides. One-hour pulse and 0-, 2-, and 5-hr chase. (C) Glycosidase digestions of the transfected cells after 20-min pulse, 1-hr chase, and immunoprecipitation. (–) Untreated; (E) Endo H; (P) PNGase F; (T) tunicamycin.

The extracellular PPT could be observed only when chase media contained 1% fetal calf serum, suggesting high sensitivity to proteolysis.

Mouse PPT has three putative N-glycosylation sites based on computer analysis with GCG's Peptidestructure program. To analyze this post-translational processing of PPT, glycosidase digestions were performed. Treatment with PNGase F or Endo H or addition of tunicamycin to the culture media yielded a single 32-kD mouse polypeptide, indicating that the different polypeptide forms are caused by differential glycosylation (Fig. 5). The Endo H sensitivity further indicates that mouse PPT does not contain complex-type sugars. After deglycosylation, mouse PPT migrated slightly more slowly than human PPT, most probably because of differences in amino acid composition.

Intracellular Localization of Mouse PPT

For immunofluorescence analysis of intracellular mouse PPT, transient transfections were performed in HeLa cells, in which the pCMV5 vector is not replicated into a high-copy plasmid. In HeLa cells, the expressed PPT was detected with rabbit polyclonal anti-human PPT and TRITC-conjugated anti-rabbit IgG antibodies, whereas the lysosomal marker lamp 1 was detected with mouse monoclonal lamp 1 antibody and FITC-conjugated anti-

mouse IgG (Fig. 6). The perinuclear punctate staining pattern colocalized with the lysosomal lamp 1 marker, indicating that like its human counterpart, mouse PPT is a lysosomal enzyme.

DISCUSSION

PPT seems to have a fundamental importance in the normal postnatal development and maturation of human neurons. The deficiency of PPT leads to the severe neurodegenerative children's disorder, INCL (Vesa et al. 1996). The striking neuropathological finding in this disease is the complete loss of cortical neurons. Currently the natural substrate for PPT is not known and the disease mechanism remains unresolved. Toward the goal of understanding the functional importance of this enzyme, we have analyzed previously the intracellular synthesis and localization of the human PPT and shown that PPT is a lysosomal enzyme (Hellsten et al. 1996). The next step in the analysis of the disease is the analysis of the mouse homolog of PPT, which offers the oppor-

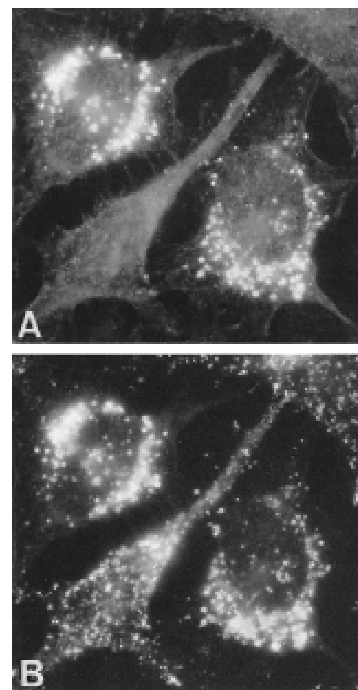


Figure 6 Intracellular localization of mouse PPT by immunofluorescence analysis. HeLa cells were transfected with mouse *PPT* cDNA and simultaneously stained with human PPT and endogenous lamp 1 antibodies. (A) Anti-human PPT antibody and TRITC-conjugated anti-rabbit IgG. (B) Lamp 1 antibody and FITC-conjugated anti-mouse IgG. In A, two *PPT*-transfected cells can be seen and the untransfected cell in the middle represents background staining.

SALONEN ET AL.

tunity to create an animal model for the disease in which the brain pathology can be studied directly.

The mouse *PPT* gene consists of nine exons spanning 21 kb of genomic DNA. The human *PPT* gene also has nine exons, but spans >26 kb because of the larger sizes of the introns (Schriner et al. 1996). The exon-intron boundaries are located at exactly the same positions. Isolation of the mouse genomic DNA allowed us to identify the chromosomal localization at chromosome 4D1-3, which is a region syntenic to human chromosome 1p32, where the human *PPT* gene has been localized (Järvelä et al. 1991). No evidence for a mouse pseudogene or another locus could be identified. The coding region of mouse *PPT* is highly homologous to human and rat *PPT* (96.3% similarity between mouse and human and 98.3% similarity between mouse and rat). No significant homology can be found in the untranslated 5' or 3' regions, suggesting that they would not have significant regulatory roles. As expected, the degree of homology between mouse, rat, and human *PPT* is highest in the characteristic thioesterase region: 100% similarity can be observed in these sequences.

Northern analysis revealed two differentially polyadenylated mouse *PPT*-specific transcripts of 2.65 and 1.85 kb in several analyzed mouse tissues. The mRNA levels are quite equal in different tissues, except in testis and kidney, in which the transcript levels were clearly higher. The steady-state mRNA levels do not correlate very well to rat *PPT* (Camp et al. 1994), except for skeletal muscle in which the lowest mRNA levels are found in both species. In each tissue except testis, the longer mRNA is more abundant, reflecting the fact that the polyadenylation site located at the end of the 1.5 kb 3'-untranslated region seems to be more efficiently utilized. The wide tissue expression of *PPT* both in mouse and humans (Schriner et al. 1996) would indicate a housekeeping role for this enzyme. On the other hand, the deficiency of *PPT* in INCL disease suggests a brain-specific substrate for this enzyme. In each case, profound analyses containing the tissue expression versus function of *PPT* still await completion.

Transient expression studies of mouse *PPT* in COS-1 cells indicated that the intracellular *PPT* is processed to mature 36/38-kD differentially glycosylated forms, is targeted lysosomally, and is partially secreted. Actually, the amount of secreted mouse *PPT* was clearly smaller than in the case of human *PPT*, because extracellular mouse *PPT* seems to be more sensitive to proteolytic degradation. This may indicate a more profound function for the ly-

sosomal *PPT* than its extracellular counterpart. Many soluble lysosomal enzymes have been reported to be secreted, especially under the circumstances of overexpression (Ioannou et al. 1992). We have not been able to detect endogenous human or mouse *PPT* in the culture medium of fibroblasts, for example (not shown), but in this case even the endogenous intracellular enzyme is difficult to detect because of the low amounts present.

The gene and predicted polypeptide structure of *PPT* as well as highly similar intracellular processing and tissue expression suggest a similar function for the mouse and human enzyme. In the future a knockout mouse model will be valuable for the studies of the molecular pathogenesis of INCL as well as for treatment trials. One naturally occurring animal model for INCL has been proposed: a lamb showing a similar severe brain disease (Palmer et al. 1986). However, no *PPT* mutations have been reported in this animal model and it remains to be seen whether it represents INCL or a closely related disease. The NCL disease family actually consists of six related diseases (infantile, three types of late infantile, juvenile, and an adult form), of which three have been shown to be caused by a defect of a lysosomal protein (Hellsten et al. 1996; Järvelä et al. 1997; Sleat et al. 1997). Once all the defective genes have been clarified, this disease family will be an interesting tool to study the normal development of neurons. Considering the techniques used today, mouse homologs of these polypeptides will be of great importance because of the small size of these animals and fast crossbreeding times.

METHODS

Isolation of the Mouse *PPT* Gene

Genomic clones were isolated from a 129 SVJ mouse liver genomic library in λ FIX II vector (Stratagene). Approximately 1×10^6 plaques were screened, using human *PPT* cDNA as a probe. Hybridization and washing conditions were performed according to standard procedures (Sambrook et al. 1989). Two clones were isolated and subcloned into the *SacI* site of the pGEM 4Z or into the *EcoRI-HindIII* and *XbaI* sites of pGEM 7Z. Subclones were sequenced using T7 and SP6 primers. Exon/intron boundaries and the sizes of introns were determined by PCR amplification of the genomic subclones using mouse *PPT* exonic primers to amplify the introns (Sambrook et al. 1989). All sequencing was performed by the dideoxy-chain termination method using T7 DNA polymerase (Sanger et al. 1977).

Fluorescence in Situ Hybridization

The cell culture from a mouse fetal tissue was established according to standard protocols (Fresney 1983) and used as a

source for metaphase chromosomes. The chromosomal localization of the mouse *PPT* gene was defined by fluorescence in situ hybridization (FISH) with a reference λ clone specific for the *COL15A1* gene (Hägg et al. 1997). To get a banding pattern on chromosomes, the cells were treated as described earlier (Tenhunen et al. 1995). The probes used to map *PPT* were a pool of three genomic subclones in pGEM4Z vectors (LM5M76, LM5M90, LM8M64; see Fig. 1) containing exons 2, 3, 4, and 5 with approximated sizes of 4.2; 2.2, and 4.0 kb. *PPT* genomic subclones were labeled with biotin-11-dUTP (Sigma Chemicals) and the *COL15A1*-specific λ clone with digoxigenin 11-dUTP (Boehringer Mannheim) by nick translation (Nick translation Reagent Kit, BRL) and detected as described elsewhere (Heiskanen et al. 1996).

RNA Analysis

Total RNA was isolated from mouse liver and brain tissues by the guanidium isothiocyanate/cesium chloride gradient method (Chirgwin et al. 1979) and used for RT-PCR analyses. Northern blot analysis was performed on Invitrogen multitissue blot filter. Hybridization with ^{32}P -labeled mouse cDNA was performed according to standard protocols (Sambrook et al. 1989). The Northern blot filter was reprobed with human β -actin to standardize the loading differences.

cDNA Cloning and Sequencing of the Mouse PPT

Two micrograms of the mouse liver and brain RNA was reverse transcribed with primer GTTCAGGCTGAGCAT-GAACTA (positions 1021–1000 on coding sequence). The cDNA was amplified by PCR with mouse-specific primers, one CAACCCAAGCTTAACAATGATGGCGTCGTCCT (positions –8 to 13) from the translation start site and another containing a *Hind*III site and TCCAACAAGCTTTCACCTAAGAAAAG-GTATGATGT (positions 922–900) upstream from the translation termination codon containing a *Hind*III restriction enzyme site. The 921-bp-long *PPT* cDNA was purified with the PCR kit (Promega), cleaved by *Hind*III, and subcloned into the *Hind*III site of the pCMV5 (Andersson et al. 1989) vector for expression in COS-1 and HeLa cells. The complete nucleotide sequence analysis of the PCR-cloned mouse *PPT* cDNA was performed by the dideoxy-chain termination method using double-stranded DNA templates.

Isolation of the 5'-Untranslated Region and Exon 1

The 5' end of the mouse genomic λ clone sequence appeared incomplete because of the absent exon 1 sequence. A sequence completing the 5' region was accomplished by PCR reaction from the mouse kidney cDNA library (gift of Vesa Olkkonen, National Public Health Institute), using a mouse *PPT* exon 4-specific primer and a T7 primer from the library vector. The amplified, 600-bp DNA fragment was purified with a PCR purification kit (Promega) and sequenced bidirectionally.

Transfection, Labeling, and Immunoprecipitation

COS-1 and HeLa cell lines were grown in Dulbecco's modified eagle medium (DMEM), supplemented with 10% fetal calf

serum and antibiotics. One day prior to transfection, cells were seeded on six-well plates, 3.5×10^5 cells per well. Transfection was performed with 5 μg of *mPPT* cDNA in pCMV5 vector, using the DEAE-dextran transfection method (Sussman and Millman 1984). Seventy-two hours post-transfection cells were pulse-labeled with [^{35}S]cysteine (Amersham) for 1 hr. For deglycosylation, tunicamycin (5 $\mu\text{g}/\text{ml}$) was added 2 hr before labeling and was used at the same concentration throughout the labeling. Cells were pulse-labeled for 2, 5, and 24 hr. The medium and the cells were collected for immunoprecipitation, which was performed with polyclonal anti-human *PPT* antibody as described previously (Hellsten et al. 1996). Immunoprecipitated *PPT* was separated on 14% SDS-polyacrylamide gels (Laemmli 1970). Endo H and PNGase F digestions were performed overnight at 37°C as described previously (Tikkanen et al. 1995).

Immunofluorescence

For immunofluorescence staining the lipofectamine (GIBCO-BRL)-transfected (Felgner et al. 1987) HeLa cells were grown on 12-mm-diam. coverslips and fixed in methanol 72-hr after transfection. Cells were double stained with anti-human *PPT* antibody and monoclonal lamp 1 antibody (gift of Vesa Olkkonen); the secondary antibodies were TRITC-conjugated anti-rabbit IgG (Immunotech) for *PPT* and FITC-conjugated antimouse IgG (Immunotech) for lamp 1. The immunofluorescence staining was visualized under a Zeiss Axiophot immunofluorescence microscopy (magnification 630 \times).

ACKNOWLEDGMENTS

We thank Tuula Airaksinen, Tuula Manninen, and Lea Puhakka for technical assistance. This study was financially supported by the Academy of Finland, the Finnish Cultural Foundation, the Hjelt Fond of the Pediatric Foundation, the Sigrid Juselius Foundation, and the Rinnekoti Research Foundation.

The publication costs of this article were defrayed in part by payment of page charges. This article must therefore be hereby marked "advertisement" in accordance with 18 USC section 1734 solely to indicate this fact.

REFERENCES

- Anderson, S., D.L. Davis, H. Dahlback, H. Jornvall, and D.W. Russell. 1989. Cloning, structure and expression of the mitochondrial cytochrome P-450 sterol 26-hydroxylase, a bile acid biosynthetic enzyme. *J. Biol. Chem.* 264: 8222–8229.
- Camp, L.A. and S.A. Hofmann. 1993. Purification and properties of the palmitoyl-protein thioesterase that cleaves palmitate from H-Ras. *J. Biol. Chem.* 268: 22566–22574.
- Camp, L.A., L.A. Verkruyse, S.K. Afendis, C.A. Slaughter, and S.L. Hofmann. 1994. Molecular cloning and expression of palmitoyl-protein thioesterase. *J. Biol. Chem.* 269: 23212–23219.
- Chirgwin, J.M., A.E. Przybala, R.J. Macdonald, and W.J. Rutter. 1979. Isolation of biologically active ribonucleic acid

SALONEN ET AL.

- from sources enriched in ribonuclease. *Biochemistry* 18: 5294–5299.
- Cowell, J.K. 1984. A photographic representation of the variability in the G-banded structure of the chromosomes in the mouse karyotype. *Chromosoma (Berl.)* 89: 294–320.
- Felgner, P.L., T.R. Gadek, M. Holm, R. Roman, H.W. Chan, M. Wenz, J.P. Northrop, G.M. Ringold, and M. Danielsen. 1987. Lipofection: A highly efficient, lipid-mediated DNA-transfection procedure. *Proc. Natl. Acad. Sci.* 84: 7413–7417.
- Fresney, I.R. 1983. *Culture of animal cells. Manual of basic technique*, p. 265. Allan R. Liss, New York, NY.
- Heiskanen, M., O.-P. Kallioniemi, and A. Palotie. 1996. Fiber-FISH: Experiences and a refined protocol. *Genet. Anal. Biol. Eng.* 12: 179–184.
- Hellsten, E., J. Vesa, V.M. Olkkonen, A. Jalanko, and L. Peltonen. 1996. Human palmitoyl protein thioesterase: Evidence for lysosomal targeting of the enzyme and disturbed cellular routing in infantile neuronal ceroid lipofuscinosis. *EMBO J.* 15: 5240–5245.
- Hägg, P.M., N.J. Horelli-Kuitunen, L. Eklund, A. Palotie, and T. Pihlajaniemi. 1997. Cloning of mouse type XV collagen sequences and mapping of the corresponding gene to 4B1-3. *Genomics* (in press).
- Ioannou, Y., D. Bishop, and R. Desnick. 1992. Overexpression of human alpha-galactosidase A results in its intracellular aggregation, crystallization in lysosomes and selective secretion. *J. Cell Biol.* 119: 1137–1150.
- Järvelä, I., J. Schleutker, L. Haataja, P. Santavuori, L. Puhakka, T. Manninen, A. Palotie, L.A. Sandkuyl, M. Renlund, R. White, P. Aula, and L. Peltonen. 1991. Infantile form of neuronal ceroid lipofuscinosis (CLN 1) maps to the short arm of chromosome 1. *Genomics* 9: 170–173.
- Järvelä, I., M. Sainio, T. Rantamäki, V.M. Olkkonen, O. Carpen, L. Peltonen, and A. Jalanko. 1997. Biosynthesis and intracellular targeting of the CLN3 protein defective in Batten disease. *Hum. Mol. Genet.* (in press).
- Laemmli, U.K. 1970. Cleavage of structural proteins during the assembly of the head of bacteriophage T4. *Nature* 227: 680–685.
- Palmer, D.N., G. Barns, D.R. Husbands, and R.D. Jolly. 1986. Ceroid lipofuscinosis in sheep. *J. Biol. Chem.* 4: 1773–1777.
- Rapola, J. and M. Haltia. 1973. Cytoplasmic inclusions in the veriform appendix and skeletal muscle in two types of so-called neuronal ceroid lipofuscinosis. *Brain* 96: 833–840.
- Sanger, F., S. Nicklen, and A.R. Coulson. 1997. DNA sequencing and chain-terminating inhibitors. *Proc. Natl. Acad. Sci.* 74: 5463–5467.
- Sambrook, J., E.F. Fritsch, and T. Maniatis. 1989. *Molecular cloning: A laboratory manual*, 2nd ed. Cold Spring Harbor Laboratory Press, Cold Spring Harbor, NY.
- Santavuori, P., M. Haltia, and J. Rapola. 1974. Infantile type of so-called neuronal ceroid lipofuscinosis. *Dev. Med. Child. Neurol.* 16: 644–653.
- Schriner, J.E., W. Yi, and S.L. Hofmann. 1996. cDNA and genomic cloning of human palmitoyl-protein thioesterase (PPT), the enzyme defective in infantile neuronal ceroid lipofuscinosis. *Genomics* 34: 317–322.
- Sleat, D.E., R.J. Donnelly, H. Lackland, C.-G. Liu, I. Sohar, R.K. Pullarkat, and P. Lobel. 1997. Association of mutations in a lysosomal protein with classical Late-Infantile Neuronal Ceroid Lipofuscinosis. *Science* 277: 1802–1805.
- Sussman, D.J. and G. Millman. 1984. Short-term, high-efficiency expression of transfected DNA. *Mol. Cell Biol.* 4: 1641–1643.
- Tenhunen, K., M. Laan, T. Manninen, A. Palotie, L. Peltonen, and A. Jalanko. 1995. Molecular cloning, chromosomal assignment, and expression of the mouse aspartylglucosaminidase gene. *Genomics* 30: 244–250.
- Tikkanen, R., N. Enomaa, A. Riikonen, E. Ikonen, and L. Peltonen. 1995. Intracellular sorting of aspartylglucosaminidase: The role of N-linked oligosaccharides and evidence of Man-6-P independent lysosomal targeting. *DNA Cell Biol.* 14: 305–312.
- Tyynelä, J., D.N. Palmer, M. Baumann, and M. Haltia. 1993. Storage of saposins A and D in infantile neuronal ceroid lipofuscinosis. *FEBS Lett.* 330: 8–12.
- Verkruyse, L.A. and S.L. Hofmann. 1996. Lysosomal targeting of palmitoyl-protein thioesterase. *J. Biol. Chem.* 28: 15831–15836.
- Vesa, J., E. Hellstein, L.A. Verkruyse, L.A. Camp, J. Rapola, P. Santavuori, S.L. Hofmann, and L. Peltonen. 1995. Mutations in the palmitoyl protein thioesterase gene causing infantile neuronal ceroid lipofuscinosis. *Nature* 376: 584–587.

Received November 4, 1997; accepted in revised form May 22, 1998.